Defects in low-temperature electron-irradiated *p*-type silicon

P. Nubile[a] and J. C. Bourgoin
Groupe de Physique des Solides de l'Université Paris 7,[b] Tour 23, 2 place Jussieu, 75251 Paris Cedex 05, France

D. Stievenard and D. Deresmes
Institut d'Electronique et de Microélectronique du Nord,[b] et Institut Supérieur d'Electronique du Nord,[b] 41, boulevard Vauban, 59046 Lille Cedex, France

G. Strobl
Telefunken System Technik, Theresienstrasse 2, 71 Heilbronn, Germany

(Received 9 April 1992; accepted for publication 1 July 1992)

Defects in monocrystalline silicon have been studied in the past, in particular, defects induced by room-temperature electron and proton irradiations on both *n*- and *p*-type materials, and most of the corresponding defects have been tentatively identified. However, there are still several questions which remain to be answered such as the nature and behavior of the defects introduced in the range 4–300 K. In this work Czochralski-grown *p*-type material has been irradiated at three different temperatures (90, 200, and 300 K) and characterized by deep-level transient spectroscopy (DLTS) and lifetime measurements. The data show that the defects created after irradiations at 90 and 200 K are different from those reported in the literature for irradiations at 4, 77, and 300 K, showing that three annealing steps exist between 4 and 300 K. These defects are characterized and a tentative identification of them is made. Finally, an attempt to detect the defects responsible for the lifetime, i.e., the recombination centers, not observed by DLTS, using spin-dependent recombination is described.

I. INTRODUCTION

Defects introduced at room temperature by electron irradiation in *p*- and *n*-type monocrystalline silicon are now well known;[1,2] however, the nature and introduction rate of the various defects created by irradiation at low temperature have not been studied in detail. The total defect introduction rate has been monitored versus the temperature of irradiation only in the case of *n*-type materials.[3] It is understood that a fraction of the created vacancy-interstitial pairs recombine at low temperature (4 K), the resulting introduction rate R being very low compared to the calculated value for the number of atomic displacements. This is probably a result of interstitial migration since in *p*-type material, an interstitial that escapes recombination exchanges its site with a substitutional acceptor impurity giving rise to an interstitial impurity.[4] When the irradiation temperature increases up to the value at which vacancies become mobile, i.e., around 100 K, R increases sharply. This is due to the fact that vacancies can then form complexes with impurities such as the dopant (E centers), oxygen (A centers), residual impurities (C in particular), while others interact with themselves forming divacancies.

In the case of *p*-type silicon no study of the variation of the introduction rate versus the irradiation temperature is available. Few experiments have been performed following irradiation at low temperature[5–9] and only the defects created at room temperature have been exhaustively studied. Table I gives the characteristics of the defect levels reported in the published works for irradiations at 300,[10] 77,[7] and 4 K (Ref. 8) in *p*-type Czochralski-grown silicon. We have modified the labels given for these levels in order to simplify their comparison with the data reported in this work. The labels we adopted are L1–L9 for the defects described in the literature and P1–P10 for the defects detected in this work.

There are five levels detected by deep-level transient spectroscopy (DLTS) following irradiation at 300 K. The L1–L4 defects are majority (hole) carrier traps, and L5 is a minority (electron) carrier trap. L2 is attributed to the divacancy (V-V), which is stable until 600 K; L3 is attributed to interstitial carbon C_I, stable until 320 K; L4 is attributed to a carbon-related complex (C_I-C_S); and L5 is a boron-related complex (B_I-B_S). L6, L7, and L8 have the same identification as L1, L2, and L3, which implies that these defects, created before the vacancy becomes mobile, are stable in the range 77–300 K; actually we shall see here that this is not the case. L9 is a level detected after irradiation at 4 K which is attributed to the isolated vacancy which becomes mobile around 90–100 K.

The aim of this study is to provide more information on the behavior of these various defects in the range 77–300 K so as to obtain a better description of the nature and concentration of the various defects introduced as a function of the temperature of irradiation, with the hope to make more precise the identifications proposed for the defects created at room temperature and to apply this knowledge to the prediction of solar-cell degradation in space. The work has been performed in boron-doped Czochralski-grown *p*-type material by means of DLTS, and lifetime- and spin-dependent recombination measurements.

[a]Permanent address: Instituto de Pesquisas Espaciais (INPE), Caixa Postal 515, CEP 12201, Sao Jose dos Campos/SP, Brazil.
[b]Laboratoires associés au Centre National de la Recherche Scientifique.

 0021-8979/92/192673-07$04.00

TABLE I. Defect labels, peak temperatures, and energy levels observed by DLTS for irradiations at different temperatures.

$T_{irradiation}$ (K)	Label in literature	T_{peak} (K)	Energy (eV)	New label	Reference
300	H1	90	0.09	L1	
	H2	120	0.21	L2	
	H3	150	0.27	L3	10
	H4	195	0.33	L4	
	E1	130	0.26	L5	
77	H(0.14)	80	0.14	L6	
	H(0.21)	125	0.21	L7	7
	H(0.27)	165	0.27	L8	
4	H(0.11)	···	0.11	L9	8
90	P1	117	0.24	···	this
	P2	160	0.22	···	work
	P3	145	0.21	···	
	P4	173	0.28	···	
200	P5	130	0.26	···	
	P6	134	0.29	···	
	P7	152	0.32	···	
300	P8	105	0.22	···	
	P9	119	0.19	···	
	P10	190	0.31	···	

II. SAMPLES AND TECHNIQUES

The samples studied are pieces of silicon solar cells for space application with a surface area of 1.24×10^{-2} cm^{-2} obtained by diamond sawing. They are $n^+/p/p^+$ structures made in Czochralski-grown wafers, where the active p layer is boron doped (as the p^+ substrate) with a nominal resistivity of 10 Ω cm. The emitter is phosphorus doped by diffusion, with a junction depth of 0.2 μm. The front and back contacts are made by Ti/Pd/Ag alloying with an Al reflector included on the rear side.

The samples were irradiated in a liquid-nitrogen cryostat allowing the irradiation temperature to be adjusted from 90 to 300 K. The beam intensities, 0.5 μA for the irradiation temperatures of 90 and 200 K, and 1 μA for the irradiation at 300 K, were chosen to keep the increase of the sample temperature below 5 K during irradiation. The irradiation doses were set to values such that the total defect concentration introduced N_T is low compared to the dopant concentration N_A (N_T/N_A)<0.1.

DLTS was performed with two types of spectrometers: a homemade one, in which the capacitance transient is analyzed with a boxcar, and another one using a capacitance meter (model PAR410) and double lock-in detection. The typical parameters used are: pulse duration 10 ms; emission rate $e_n=20$ s^{-1}; reverse bias: −2 V. The pulse amplitude was such that the bias is 0 V for the study of majority-carrier traps, and +0.5 V for the study of minority-carrier traps. These parameters were kept constant when comparing the spectra obtained for the different temperatures of irradiation.

The defect energy levels were obtained from the slopes of the plot of $\ln(e_nT^{-1})$ vs T^{-1} and the concentrations deduced from the amplitudes of the DLTS peaks. The change Δp in the total free-hole concentration p is obtained from the change in capacitance:

$$\Delta p=p-p_0=p_0[1-(C/C_0)^2], \tag{1}$$

where p_0 and C_0 are the total free-carrier concentration and capacitance before irradiation, respectively, and p and C are the values of these parameters after irradiation. By means of Eq. (1) the total introduction rate R was calculated for each irradiation temperature.

The cross sections σ_n associated with the minority-carrier traps were deduced from the filling kinetics. In this case one can write

$$n_T(t_p)=N_T[1-\exp(-c_nt_p)], \tag{2}$$

where n_T is the concentration of filled traps after a filling pulse of a given duration t_p, N_T the total trap concentration, and c_n the capture rate. The concentration of filled traps is obtained by means of the capacitance peak amplitude as follows:

$$n_T/N_A=2\Delta C/C, \tag{3}$$

where ΔC is the amplitude of the DLTS peak. Once the capture coefficient c_n is determined, the capture cross section is obtained by

$$\sigma_n=c_n(nv)^{-1}, \tag{4}$$

where n is the injected carrier concentration during the filling pulse and v is the thermal electron velocity.

The injected carrier concentration n is related to the current J that flows through the junction during the filling pulse, the lifetime τ, and the diffusion coefficient D_n through

$$n=J(\tau/D_n)/q, \tag{5}$$

where q is the electronic charge.

The lifetime τ was measured using the Kingston's method[11] which consists in measuring the current transient through a p-n junction starting from a direct polarization current, J_F to a reverse polarization current J_R. When $J_F=J_R$, the storage time of the minority carriers t_s is directly related to the lifetime through

$$\tau=4.4t_s. \tag{6}$$

The parameters used for the measurements were: $J_F=J_R=0.5$ A cm^2 and a pulse duration of 100 μs. At room temperature the lifetime and diffusion coefficient have typical values of 50 μs and 100 cm^{-2} s^{-1}, respectively. With these values the injected carrier concentration is of the order of 10^{14} cm^3 when keeping the diode in the low injection condition.

Since, as we shall see, it has not been possible to observe the defects responsible for this lifetime (the recombination centers having energy levels located in the middle of the gap), an attempt has been made to detect[12] them by spin-dependent recombination (SDR). This technique allows the electrical detection of recombination centers located in the space charge of a junction, by electron paramagnetic resonance (EPR). It therefore combines the

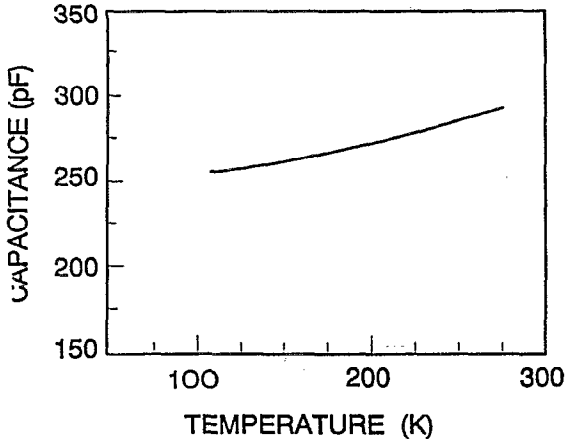

FIG. 1. Capacitance vs temperature in unirradiated samples measured under 0 V bias.

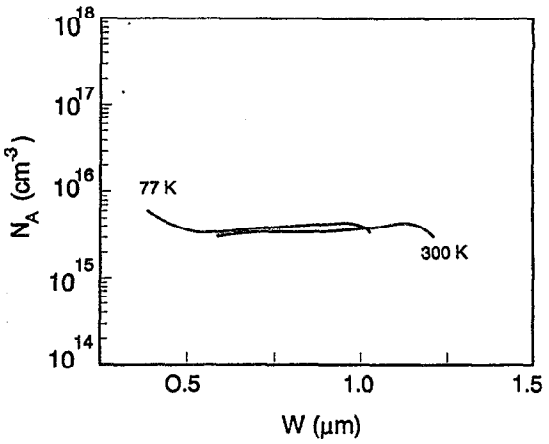

FIG. 3. Uncompensated hole concentration vs depth calculated from the curves of Fig. 2 for 300 and 77 K.

sensitivity of the electrical techniques with the potentialities of EPR regarding the microscopic information this last technique provides. The principle of SDR is to modify the process of carrier capture by a change of the defect spin population, inducing at magnetic resonance, a variation of the recombination current of a diode biased under low forward voltage. We used an *X*-band spectrometer with the diode biased at 0.1 V and we detected, through a lock-in detector, the variation (few pA) of the forward current ($\sim$1 μA). The microwave power used was 200 mW and the modulation of the magnetic field was 6 kHz.

III. RESULTS

A. Characterization before irradiation

A characterization before irradiation is necessary to determine the parameters of reference, such as the impurity concentration p_0 and the room temperature lifetime τ_0. The capacitance as a function of temperature, measured under 0 V bias, is given in Fig. 1. The capacitance voltage characteristics at 300 and 77 K are given in Fig. 2. The depth explored is different at 77 and 300 K because the built-in voltage of the diode varies with temperature (from 0.6 V at 300 K to 0.8 V at 77 K). The uncompensated hole concentrations are identical (2×10^{15} cm^{-3}) at 300 and 77 K, as can be seen in Fig. 3. This value of hole concentration gives a base resistivity of 8 Ω cm in the Irvin curve[13] which is therefore in agreement with the nominal base resistivity of the material.

Figure 4 shows the lifetime in the range 100–300 K: It varies approximately linearly with temperature from 40 μs at 300 K to 1 μs at 100 K. The variation of ln τ vs $1000/T$, given in Fig. 5, indicates that the lifetime is governed by a defect having a minority-carrier cross section characterized by an electron capture barrier of 50 meV. This defect, however, is not detected by DLTS, presumably because it corresponds to an electron emission occurring above 300 K. DLTS measurements in the range 77–300 K do not detect any majority or minority-carrier trap before irradiation.

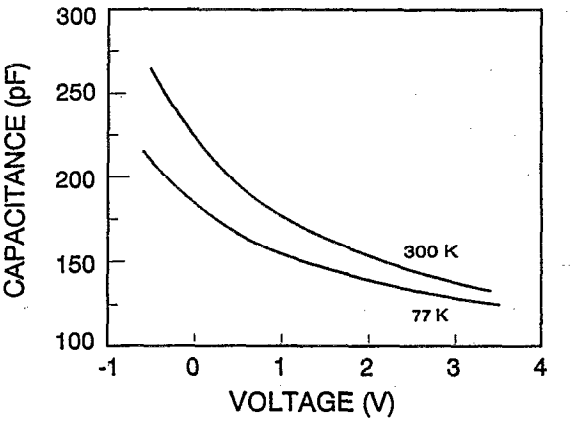

FIG. 2. Capacitance vs voltage in unirradiated samples measured at 300 and 77 K.

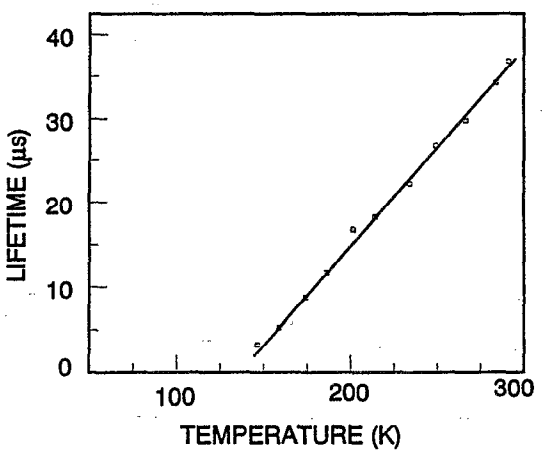

FIG. 4. Lifetime vs temperature in unirradiated samples.

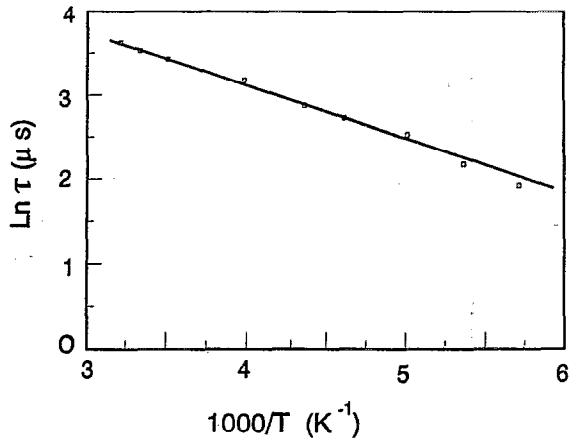

FIG. 5. ln τ vs the inverse of the temperature in unirradiated samples.

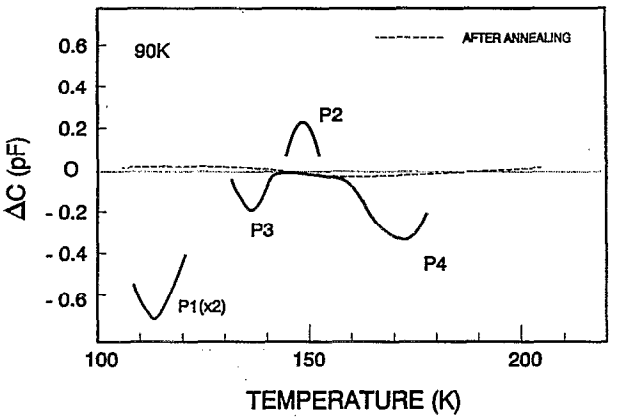

FIG. 6. DLTS spectrum obtained after irradiation at 90 K (solid line) and annealing at room temperature (dashed line).

B. Characterization after irradiation

The total defect introduction rates produced by 1 MeV electron irradiation at 90, 200, and 300 K are given in Table II. Assuming that the free holes removed by the irradiation are trapped by the induced defects, this table shows that the introduction rate R increases with temperature, as in the case of n-type material, with a comparable magnitude.

The DLTS spectra obtained for these three irradiation temperatures are given in Figs. 6–8 together with the spectra obtained after room temperature annealing during 1 h. The spectra of minority-carrier traps are given after extraction by difference with the spectra experimentally obtained, i.e., containing both minority- and majority-carrier peaks.

The signatures of the various peaks are given in Fig. 9 for the majority-carrier traps and in Fig. 10 for the minority-carrier traps. Table III provides the values of the corresponding energy levels ΔE above the valence band for the majority-carrier traps and below the conduction band for the minority-carrier traps and their apparent cross section σ obtained from the extrapolation of the signature when $1000/T$ tends to zero, together with the corresponding introduction rates.

The lifetimes τ after irradiation were measured for samples irradiated at room temperature with doses ranging from 1×10^{13} to 5×10^{15} cm^{-2} because, for higher doses, the lifetime was too short to be measured accurately. Figure 11 shows that the introduction of recombination centers varies linearly with the dose. This curve gives the irradiation coefficient K_τ, defined as

$$(1/\tau)-(1/\tau_0)=K_\tau\Phi, \tag{7}$$

where τ_0 is the lifetime before irradiation. The lifetime extrapolated for a higher dose is then obtained from the knowledge of K_τ (1.9×10^{-9} cm^2 s).

The determination of the minority trap concentration was made with the help of the curves shown in Fig. 12, which gives the variation of the capacitance change as a function of the forward applied voltage for two filling pulse durations (50 and 100 μs). The curves show that there is a saturation of the minority-carrier traps: Over this value there are no available defects to trap the exceeding carriers. This level therefore corresponds to the concentration for the minority-carrier traps.

IV. DISCUSSION

The data of Table II show that the defect introduction rates decrease with decreasing irradiation temperature; but, for all of the defects it remains in the range of 10^{-3}–10^{-2} cm^{-1}.

Irradiation performed at 90 K induces three majority traps (P1, P3, and P4) and one minority trap (P2). All these defects are annealed at room temperature. They are not identical to those already detected for irradiations at a slightly lower temperature. Kimerling and co-workers[7] give defect spectra and isochronal annealing data for 1 MeV irradiation at 77 K. They also observed three majority peaks (L6, L7, and L8; see Table I). Apparently, no minority-carrier trap was searched for in this work. The majority peak L6, also observed after 4 K irradiation [label

TABLE II. Capacitance after C and before irradiation C_0, majority-carrier concentration before irradiation p_0, its variation Δp after irradiation, total fluence Φ, and introduction rate R for samples irradiated at 90, 200, and 300 K.

$T_{\text{irradiation}}$ (K)	C (pF)	C_0 (pF)	p_0 (cm^{-3})	Δp (cm^{-3})	Φ (cm^{-2})	R (cm^{-1})
90	132	130	3×10^{15}	9.0×10^{13}	1×10^{16}	9.0×10^{-3}
200	136	133	3×10^{15}	1.3×10^{14}	5×10^{15}	2.6×10^{-2}
300	147	140	2×10^{15}	1.8×10^{14}	5×10^{15}	3.6×10^{-2}

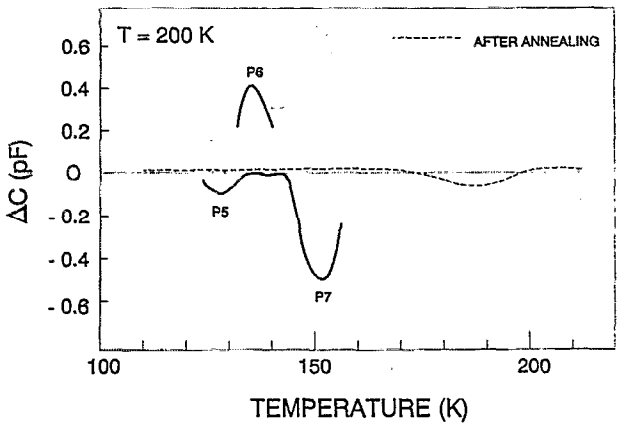

FIG. 7. DLTS spectrum obtained after irradiation at 200 K (solid line) and annealing at room temperature (dashed line).

(a)], by Brabant *et al.* using thermally stimulated capacitance data,[8] and by Watkins and co-workers,[6] is attributed to the isolated vacancy. The peak L7 is attributed to the divacancy and L8 is attributed to a carbon interstitital.

Although occurring near the same temperature in the DLTS spectrum, the trap P1 found in this work is different from trap L9 (L6) detected after an irradiation of 2.4–3 MeV electrons at 4.2 K. Figure 13 compares the signatures for these levels, which demonstrate that they do not correspond to the same trap. On the other hand, trap P1 cannot be associated with L7 (having a similar ionization energy) because of its relative concentration in relation to the other traps and its annealing characteristics. The DLTS level of P1 is about four times the level of the minority peak trap P2. Instead, in Ref. 10; this ratio may be inverted. Also, the peak L7 has its concentration increasing with the annealing temperature, in contradiction with our annealing data shown in Fig. 6. Thus, because we do not observe trap L6 (L9), this means that at 90 K under irradiation the vacancy is already mobile.

Since all defects have disappeared after increasing the temperature to 300 K, this means that the traps we detected here cannot be associated with divacancies or interstitial impurities. Indeed, a divacancy anneals around 600 K and an acceptor interstitial around 700 K. Consequently, trap L7 cannot be attributed to the divacancy since all the traps we observe at 90 K are annealed at 300 K. The vacancies being mobile during irradiation at 90 K, they should interact with impurities giving rise to unknown *V-X* complexes. Consequently, P1, P2, P3, and P4 are lev-

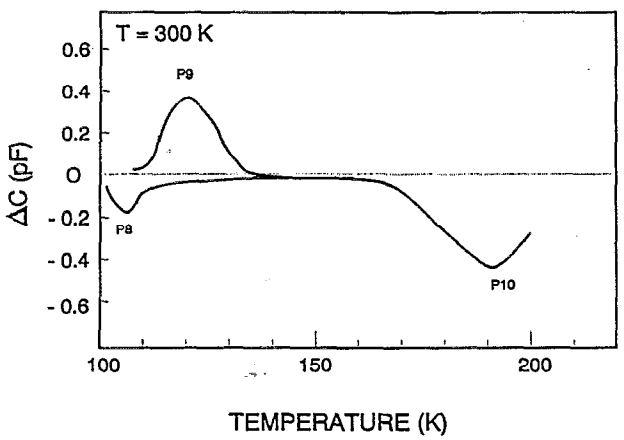

FIG. 8. DLTS spectrum obtained after irradiation at 300 K.

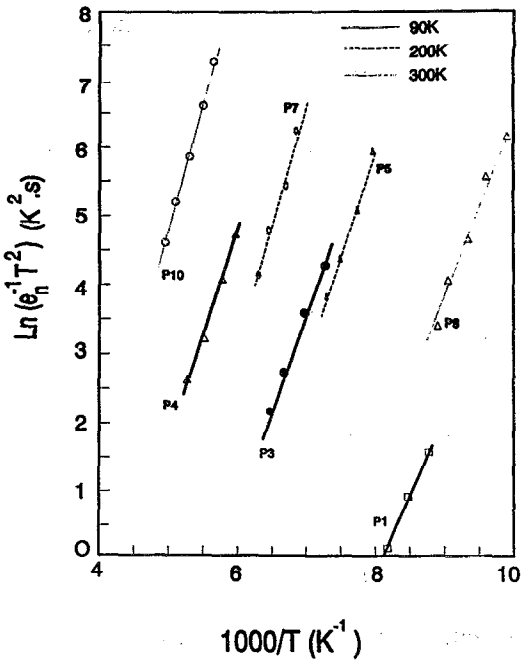

FIG. 9. Signatures (variation of the emission rate vs temperature) of the majority traps observed after irradiation at 90, 200, and 300 K.

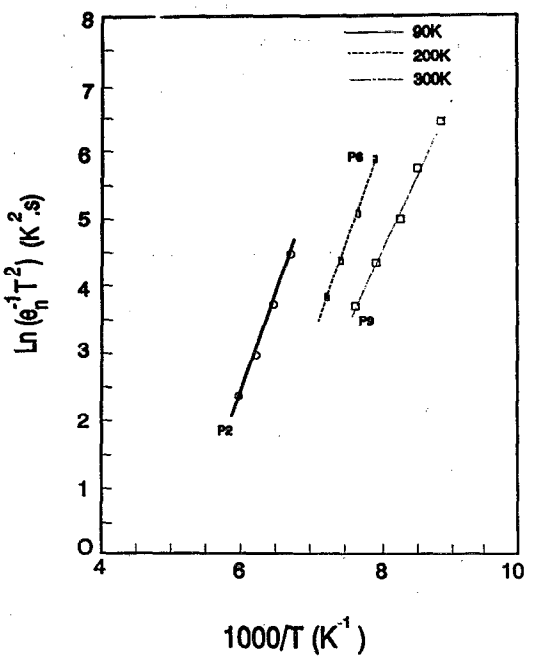

FIG. 10. Signatures (variation of the emission rate vs temperature) of the minority traps observed after irradiation at 90, 200, and 300 K.

TABLE III. Label, peak temperature T_{max}, capacitance variation $\Delta C/C_0$, introduction rate R, energy level ΔE, and apparent cross section σ.

Label	T_{max} (K)	$\Delta C/C_0$	R (cm^{-1})	ΔE (meV)	σ (cm^2)
P1	117	1.1×10^{-3}	6.6×10^{-2}	244	2×10^{-10}
P2	160	1.9×10^{-3}	1.1×10^{-3}	216	4×10^{-15}
P3	145	1.4×10^{-3}	0.8×10^{-3}	209	9×10^{-15}
P4	173	2.2×10^{-3}	1.3×10^{-3}	282	4×10^{-14}
P5	130	7.3×10^{-4}	1.5×10^{-3}	261	2×10^{-12}
P6	134	3.3×10^{-3}	6.6×10^{-3}	286	1×10^{-11}
P7	152	2.9×10^{-3}	5.8×10^{-3}	319	3×10^{-12}
P8	105	1.2×10^{-3}	0.7×10^{-2}	218	3×10^{-12}
P9	119	2.6×10^{-3}	1.6×10^{-2}	191	8×10^{-15}
P10	190	2.9×10^{-3}	1.7×10^{-2}	305	4×10^{-15}

els associated with different V-X complexes. The impurities X involved are neither the doping impurity nor O since the E and A centers are stable at room temperature.

Irradiation performed at 200 K shows similar trends. There are two majority peaks (P5 and P7) and one minority peak (P6). After annealing at 300 K a peak around 200 K appears. This peak is presumably the peak L8 found after irradiation at room temperature. These results show that defects P5 and P6 are probably also complexes (V-X) involving the vacancy.

Irradiation performed at 300 K shows the well-known H2, E1, and H3 defects labeled here P8, P9, and P10 (see Table I). These traps again exhibit characteristics different from the traps obtained after 200 K irradiation which implies that annealing takes place in the range 200–300 K.

Thus, the different DLTS spectra obtained after 90, 200, and 300 K irradiations demonstrate that there are at least three annealing steps: between 4 and 90 K, between 90 and 200 K, and between 200 K and room temperature. This is partially in agreement with the observations of Brabant *et al.*,[8,9] who observed three annealing steps at 53, 82, and 110 K.

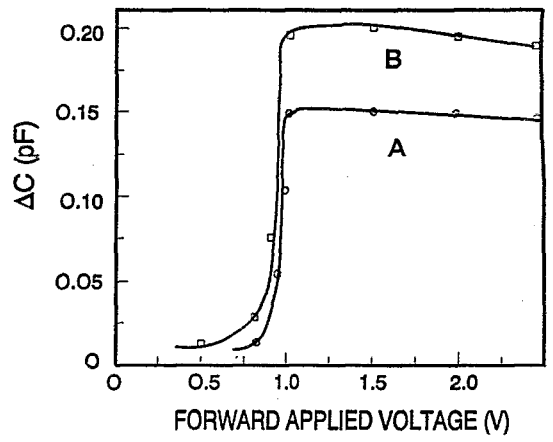

FIG. 12. Variation of the amplitude of the minority peak as a function of the forward current for pulse durations of (a) 50 and (b) 100 μs.

V. SPIN-DEPENDENT RECOMBINATION

The samples used in this work were silicon solar cells for space applications. For these samples, the minority-carrier peak could be of special interest, because the main solar-cell characteristics are governed by the minority-carrier transport parameters as the lifetime and the diffusion length. The cross sections for the minority-carrier traps were measured for the sample irradiated at 90 and 300 K. For the 300 K irradiation, we found for the minority trap (P9) $\sigma_n=3\times10^{-18}$ cm^2 and for the 90 K irradiation (trap P2), $\sigma_n=1\times10^{-20}$ cm^2. These results show that the contribution of these minority traps to the effective minority-carrier lifetime is negligible since they correspond to lifetimes very large compared to the measured value.

It thus appears that conventional DLTS used so far does not probe the defects responsible for lifetime degradation. DLTS coupled with annealing studies only helps in the identification of the created defects but does not allow the study of recombination centers.

Consequently, we have attempted to detect such defects by SDR in a sample irradiated at room temperature

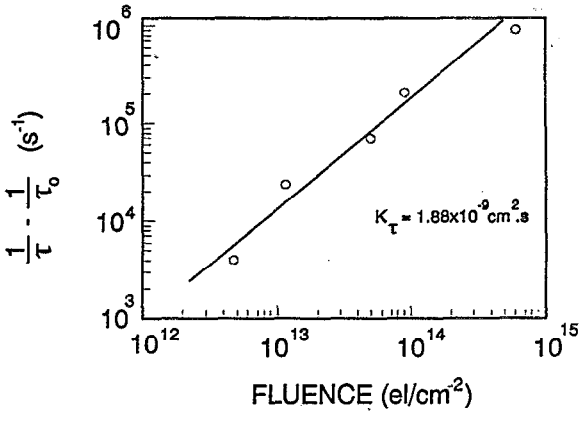

FIG. 11. Variation of $(1/\tau)-(1/\tau_0)$ vs fluence for samples irradiated at 300 K.

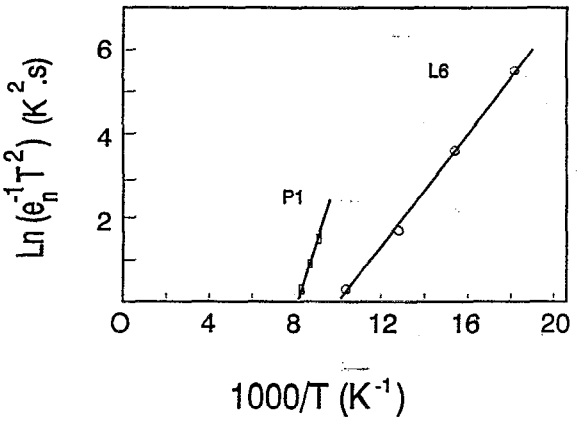

FIG. 13. Comparison of the signatures of peaks P1 (0.21 eV) found after irradiation at 90 K and of peak L6.

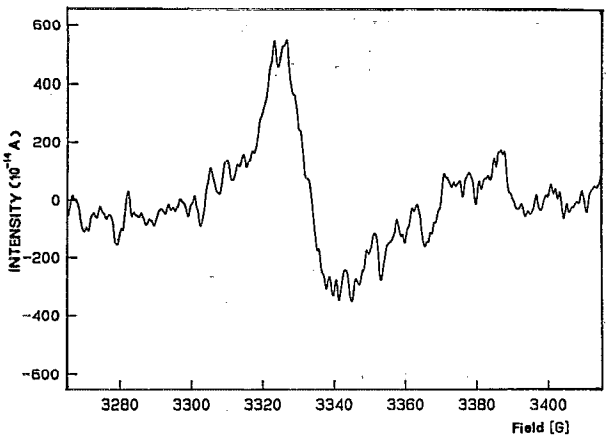

FIG. 14. Electron paramagnetic spectrum detected by spin-dependent recombination in a sample irradiated with 5×10^{15} cm^{-2}.

with 5×10^{15} e cm^{-2}. Figure 14 shows the spectrum obtained, not present before irradiation. It exhibits a g factor of 2.0036 and corresponds to a spin concentration in the range 10^{12}–10^{13} cm^{-3}. The spectrum is rather broad and the hyperfine interaction cannot be resolved. The corresponding defect can well be the one dominating the lifetime since it would correspond to a cross section of $\sim10^{-14}$ cm^2 to account for the lifetime ($\sim10^{-7}$ s) measured in this sample. Although it cannot be identified, due to the lack of detection of the hyperfine interactions, this defect could well be the divacancy (i.e., correspond to one of the associated levels) which is known to exhibit the same g value.[14]

VI. CONCLUSION

DLTS analysis of irradiated p-type monocrystalline silicon at 90 and 200 K shows the existence of new defects, i.e., of defects that have not been yet detected for irradiations at 4 or at 300 K, which must be complexes between the vacancy and residual impurities. Since these defects are all annealed out at 300 K, this implies that there are two annealing stages between 90 and 200 K and 200 and 300 K. It thus appears that the behavior of electron-induced defect in Si is more complicated than previously admitted. This leads to questions concerning the identification so far proposed and accepted of some of the defects created by irradiation at room temperature.

ACKNOWLEDGMENTS

This work has been partly supported by an ESA/ESTEC Contract No. 9190/90/NL/VS(SC). The authors are grateful to K. Bogus, M. Martella (ESA/ESTEC), and K. Roy (Telefunken) for helpful discussions.

[1] I. Weinberg and C. K. Swartz, 14th IEEE Photovoltaic Specialists Conference, 1980, p. 858.
[2] P. J. Drevinsky, H. M. De Angelis, J. T. Schott, and W. P. Rahilly, 14th IEEE Photovoltaic Specialists Conference, 1980, p. 835.
[3] H. J. Stein, in *Radiation Effects in Semiconductors*, edited by J. W. Corbett and G. D. Watkins (Gordon and Breach, New York, 1971), p. 125.
[4] G. D. Watkins, in *Radiation Damage in Semiconductors*, edited by P. Baruch (Dunod, Paris, 1965), p. 97.
[5] P. Vajda and L. J. Cheng, in *Radiation Damage and Defects in Semiconductors* (The Institute of Physics, London, 1973), p. 245.
[6] G. D. Watkins, J. R. Troxell, and A. P. Chatterjee, Int. Phys. Conf. Ser. **46**, 16 (1979).
[7] L. C. Kimerling, P. Blood, and W. M. Gibson, Int. Phys. Conf. Ser. **46**, 273 (1979).
[8] J. G. Brabant, M. Pugnet, J. Barbolla, and M. Brousseau, J. Appl. Phys. **47**, 4809 (1976).
[9] J. G. Brabant, M. Pugnet, J. Barbolla and M. Brousseau, Int. Phys. Conf. Ser. **31**, 200 (1977).
[10] L. C. Kimerling, Int. Phys. Conf. Ser. **31**, 221 (1977).
[11] R. H. Kingston, Proc. IRE **42**, 829 (1954).
[12] D. Lepine, Phys. Rev. B **6**, 435 (1972).
[13] J. C. Irvin, Bell Syst. Tech. J. **41**, 387 (1962).
[14] G. D. Watkins and J. W. Corbett, Phys. Rev. **138**, A543 (1965).